ON THE DEVELOPMENT OF 18-45 GHZ ANTENNAS FOR TOWED DECOYS AND SUITABILITY THEREOF FOR FAR-FIELD AND NEAR-FIELD MEASUREMENTS

Matthew Radway, Nathan Sutton, Dejan Filipovic

University of Colorado, 425 UCB
Boulder, Colorado 80309-0425

Stuart Gregson, Kim Hassett
Nearfield Systems, Inc.
19730 Magellan Drive
Torrance, CA 90502-1104

ABSTRACT

The development of a wideband, high-power capable 18-45 GHz quad-ridge horn antenna for a small towed decoy platform is discussed. Similarity between the system-driven antenna specifications and typical requirements for gain and probe standards in antenna measurements (that is, mechanical rigidity, null-free forward-hemisphere patterns, wide bandwidth, impedance match, polarization purity) is used to assess the quad-ridge horn as an alternative probe antenna to the typical open-ended rectangular waveguide probe for measurements of broadband, broad-beam antennas. Suitability for the spherical near-field measurements is evaluated through the finite element-based full-wave simulations and measurements using the in-house NSI 700S-30 system. Comparison with the near-field measurements using standard rectangular waveguide probes operating in 18-26.5 GHz, 26.5-40 GHz, and 33-50 GHz ranges is used to evaluate the quality of the data obtained (both amplitude and phase) as well as the overall time and labor needed to complete the measurements. It is found that, for AUTs subtending a sufficiently small solid angle of the probe's field of view, the discussed antenna represents an alternative to typical OEWG probes for 18-45 GHz measurements.

Keywords: Far-Field, Near-Field, Probe, Waveguide, Modeling

1.0 Introduction

The 1-110 GHz antenna testing facility at the University of Colorado Boulder was designed and built by Nearfield Systems Inc. and is based on the NSI-700S-30 spherical near-field scanner [1]. Field probing in the 1-50 GHz range is accomplished by ten open-ended waveguide (OEWG) probes sized from WR-650 to WR-22. While the system is versatile and capable of measuring a wide variety of antennas, the types of antennas most frequently tested using this facility are small, broad-beam, wideband antennas, with bandwidths usually exceeding two octaves and beamwidths often in excess of 60 degrees.

Of interest in the current research effort is the antenna development in 18-45 GHz frequency range. To cover this range, the previously-described system requires three probes and two manual range RF configurations. This paper discusses the tradeoffs between the labor, measurement time reductions, and measurement accuracy when the functions of the three probes are consolidated to a single probe.

The paper is organized as follows: First, we discuss some general characteristics of an AUT, which is representative of antennas typically measured in the testing facility. Second, comparison of numerical analysis results for both the OEWGs and a candidate quad-ridge horn (QRH) probe are discussed. Finally, the OEWGs and QRH are compared using the unprocessed spherical near-field measurement data of the AUT.

2. Antenna Under Test (AUT)

Recently the antenna testing facility has been mainly used for the development of wideband electronic support (ES) and electronic attack (EA) antennas covering an aggregate bandwidth of 1-110 GHz. Typical examples are planar spiral, sinuous, and log-periodic antennas, LPDAs, ridged horns, and small arrays thereof.

A representative example of such an antenna is a quad-ridged horn antenna intended for towed decoy application [2]. This antenna has a nominal beamwidth of 60°, and covers the 18-45 GHz band. It utilizes a uniformly-illuminated quad-ridged aperture, which is not often used in conjunction with broad-beam horn antennas. Most broad-beam horns increase the beamwidth by introducing aggressive flaring from the throat to the aperture, which increases the aperture phase error. However, this flaring typically results in a large aperture size, which is at odds with the objective to minimize the antenna's footprint on

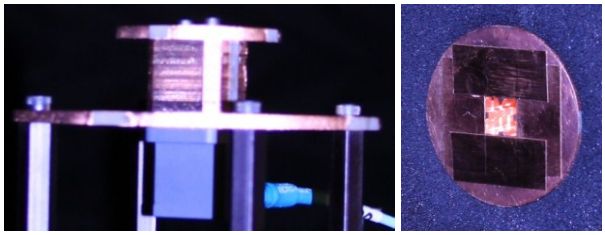

(a) Bench testing (b) Pattern testing

Figure 1 – A representative antenna under test (AUT). (a) Side view in bench testing configuration and (b) end view of pattern testing configuration.

the space-constrained decoy platform. Additionally, the taper needed to realize this flaring is often at odds with the requirement to minimize the antenna length.

An alternative approach was used where beam broadening is accomplished by constraining the aperture dimensions. Loading the aperture with ridges allows further size reduction by lowering the cutoff frequency of the desired mode. Due to field coupling to the ridges, the E-plane ridges tend to constrain the E-plane beamwidth, while the H-plane ridges constrain the H-plane beamwidth. The aggressiveness of ridge loading is further constrained by the desire that the aperture have VSWR < 2:1 throughout the 18-45 GHz bandwidth.

The aperture is fed by a double ridge waveguide cross-section modified to achieve single-mode operation beyond the 18-45 GHz bandwidth. The transition to the aperture is accomplished by a gradual 1inch (2.54 cm) long linear taper, which introduces only a small amount of aperture phase error.

While the prototype can be realized by many methods, to reduce cost and fabrication time a PCB stacking technique was used to realize the antenna. The waveguide-to-aperture taper consists of several plated slots stacked vertically as shown in Figure 1. As mounted for pattern testing the AUT has a maximum radial extent (MRE) of no more than eight inches from the origin of the AUT coordinate system. For a measurement radius of approximately 84 inches (213.36cm) this corresponds to a subtended angle of less than 6 degrees as seen by the probe.

3. Modeling results: Rectangular Open-Ended Waveguide (OEWG) vs. Quad-Ridged Horn (QRH)

A refinement of the AUT fabricated by wire Electric Discharge Machining (EDM) is used as the probe antenna. The uncorrected probe model assumes that the probe has a pure-polarized isotropic amplitude pattern with an isotropic (i.e. spherical) phase front, conditions that cannot be satisfied by a physical antenna. While in the most general case probe correction is needed to

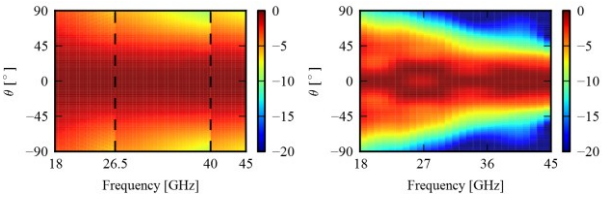

(a) WR-42,-28,-22 OEWGs (b) QRH

Figure 2 - E-plane patterns (units – dB)

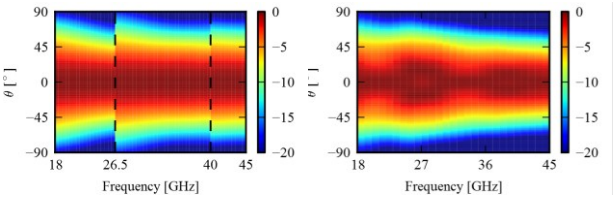

(a) WR-42,-28,-22 OEWGs (b) QRH

Figure 3 - H-plane patterns (units – dB)

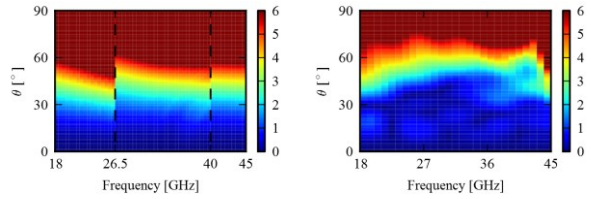

(a) WR-42,-28,-22 OEWGs (b) QRH

Figure 4 - Conical-cut pattern variation versus broadside angle (units – dB)

deconvolve the probe response from that of the AUT, this correction can be omitted if the errors are sufficiently small [3]. Since the typical AUTs subtend a small solid angle of the probe, the comparisons in the remainder of this paper presuppose that probe correction is not used.

A. Amplitude Patterns Figures 2 and 3 show the HFSS-simulated [4] OEWG and QRH E- and H-plane patterns respectively, where it is evident that the QRH has more nearly equal E- and H-plane beamwidths than the OEWG. The choice of a four-fold symmetric aperture with optimization of the ridge dimensions is the cause of this characteristic. Spherical mode decomposition in FEKO shows that modes other than $\mu=\pm1$ are 31, 19, and 16 dB down at the low, middle, and high portions of the 18-45 GHz spectrum, indicating that probe correction is possible and that the QRH is generally suitable for spherical near field measurements. On the other hand, the OEWG is smoother and more stable. Whereas the OEWG knife-edge aperture edge treatment helps suppress diffraction, by contrast the larger QRH body supports radiating currents that contribute small amounts of contamination to the radiation pattern, including the approximately 1 dB E-plane bifurcation observed near 27 GHz. This effect could be minimized if the knife-edge treatment is adopted for the QRH.

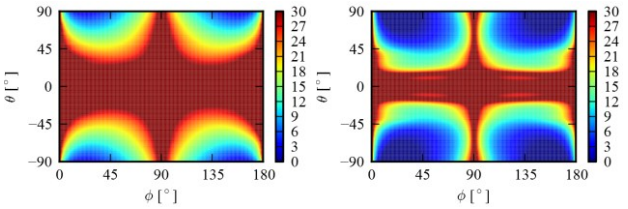

(a) WR-28 OEWG (b) QRH

Figure 5 – Mid-band cross-polarization discrimination (XPD) patterns (units – dB)

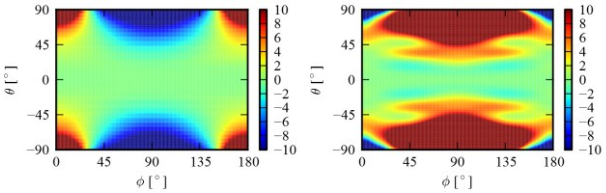

(a) WR-28 OEWG (b) QRH

Figure 6 – Mid-band phase patterns (units – deg)

B. WoW Patterns The gain variation along a conical cut about the *z* (broadside) axis (known as WoW) of the OEWG and QRH antenna is shown in Figure 4. Since the E- and H-plane beamwidths have been equalized, the WoW of the QRH is lower than that of the OEWG. The low WoW is highly desirable for the towed decoy application since it implies good beam symmetry, and improves performance as a near-field probe.

C. XPD Patterns Based on reasoning often used in reflector feed design, the fact that the E- and H-plane beamwidths are equalized would seem to imply that the cross-polarization discrimination (ratio of co-pol gain to cross-pol; XPD) field-of-view (FOV) would be better for the QRH. However, the presence of the ridges introduces cross-polarized field components into the antenna aperture, thereby reducing the 30 dB XPD FOV (Figure 5) from about 60° to less than 30°.

D. Phase Patterns As mentioned earlier, the ideal probe phase front is spherical with the origin centered on the probe aperture. While the OEWG patterns are smooth, the QRH amplitude pattern undulation discussed earlier hints at the presence of underlying phase nonuniformity, which is borne out in Figure 6b. However, there is a band near broadside where the phase is essentially uniform.

E. Phase Center The phase center *z* axis displacement from the aperture face is calculated over a 60° beamwidth using the algorithm in [5] and results are shown in Figure 7. In both cases the phase center can be seen to be stable, with OEWG outperforming QRH in all bands. The *x* and *y* displacements are zero as dictated by the pattern symmetry.

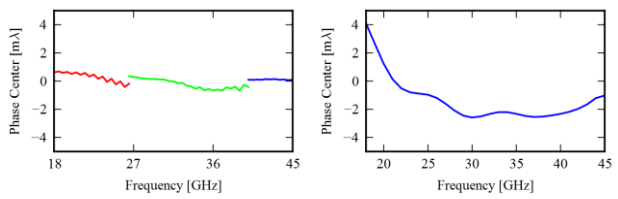

(a) WR-42,-28,-22 OEWGs (b) QRH

Figure 7 – Phase center displacement from aperture face

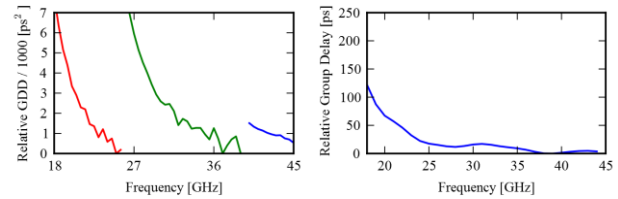

(a) WR-42,-28,-22 OEWGs (b) QRH

Figure 8 – Broadside relative group delay

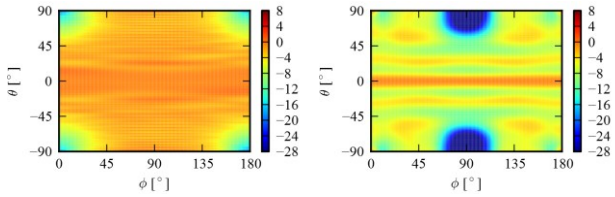

(a) WR-28 OEWG (b) QRH

Figure 9 – Mid-band group delay pattern (units - ps)

F. Group Delay Variation In UWB applications it is desirable that the group delay vary little versus frequency, so that all signal frequency components arrive together. Figure 8 shows that the group delay for the QRH is generally flatter than for the OEWG composition. This makes sense because the QRH has only one cutoff frequency (where group delay varies fastest). Figure 9 shows the group delay pattern uniformity, where it is evident that the OEWG is more uniform. Since uniformly-distributed group delay is easier to correct, the OEWG is preferable in situations where this parameter is of concern.

G. Group Delay Dispersion (GDD) Taking the frequency derivative of the group delay yields the group delay dispersion, shown in Figures 10 and 11. As seen, both the broadside and pattern GDDs are lower for the QRH.

4. Measurement Comparison

Since the performances of the OEWG and QRH are very similar near broadside, and the AUT subtended angle is small, it was assumed that the differences between pattern measurements conducted with the QRH and the OEWG

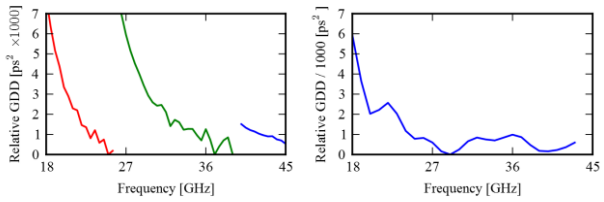

(a) WR-42,-28,-22 OEWGs (b) QRH

Figure 10 – Broadside relative group delay dispersion

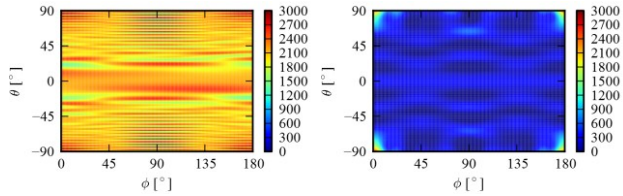

(a) WR-28 OEWG (b) QRH

Figure 11 – Mid-band group delay dispersion (units – ps^2)

would be acceptably small. A test measurement was then conducted to compare the two probe styles. Figures 12 and 13 compare unprocessed spherical near-field data taken with the two probe styles and the far-field patterns predicted by *HFSS*. It can be readily seen that the differences between the measurements are much smaller than the differences with the computational model, indicating excellent agreement between the two. The noise observed in the QRH patterns at 18 GHz is the subject of investigation, but QRH mismatch and physical range configuration have been ruled out as contributors.

The co-polarized component amplitude error is shown in Figure 14, which is obtained by subtracting the normalized amplitudes and plotting in decibels. The error is generally less than -10 dB, decreasing near broadside and with increasing frequency. The co-polarized component phase error is shown in Figure 15, which is obtained by subtracting the broadside-normalized phases. As expected, the agreement generally improves toward broadside and with increasing frequency. The 18 and 27 GHz OEWG and QRH measurements were performed 17 months apart, indicating good repeatability. The 36 and 45 GHz measurements were performed the same week.

Based on these measured results it is clear that the QRH probe performs on par with the three OEWG probes, while reducing setup time, measurement time, and component wear. Table I summarizes the time savings realized by the use of the broadband QRH as compared to three OEWG probes. While for typical AUTs the scan time dominates the total measurement time, the two saved probe change cycles represent a significant reduction in labor cost.

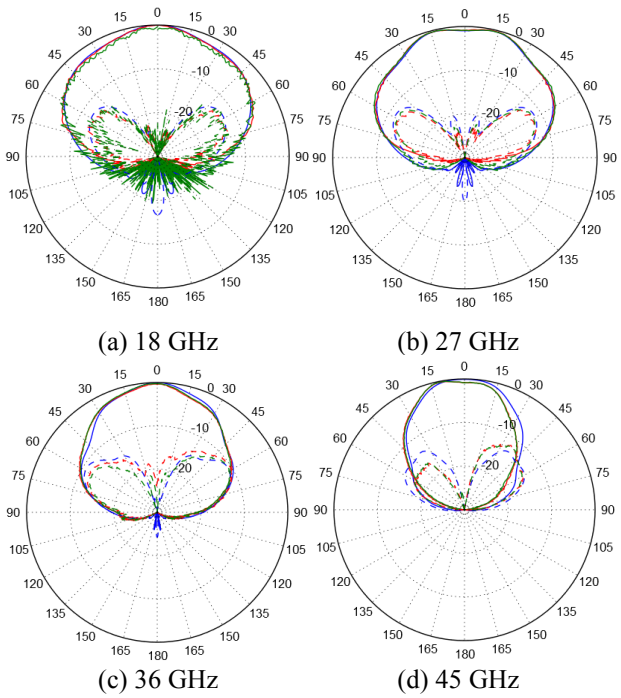

(a) 18 GHz (b) 27 GHz

(c) 36 GHz (d) 45 GHz

Figure 12 – 45° diagonal normalized elevation amplitude patterns. Data traces are as follows: red, WR-22 probe; green, QRH probe; blue, HFSS.

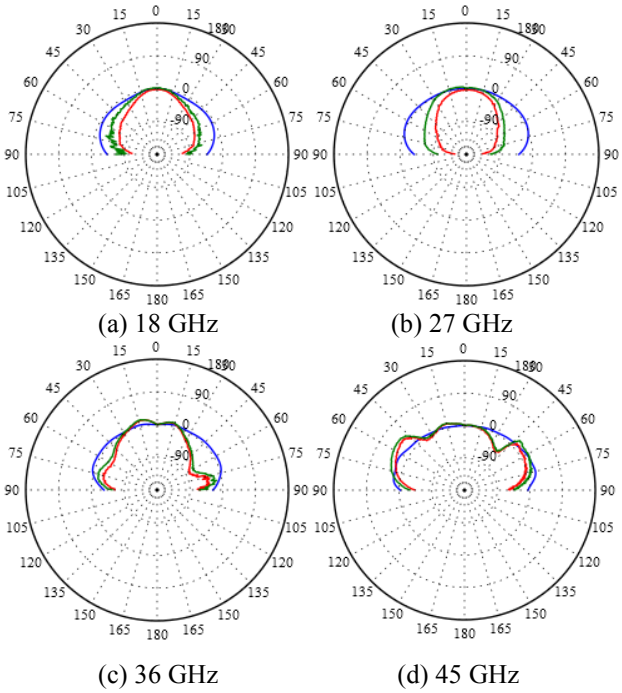

(a) 18 GHz (b) 27 GHz

(c) 36 GHz (d) 45 GHz

Figure 13 – H-plane normalized elevation phase pattern comparison. Data traces are as in Figure 12.

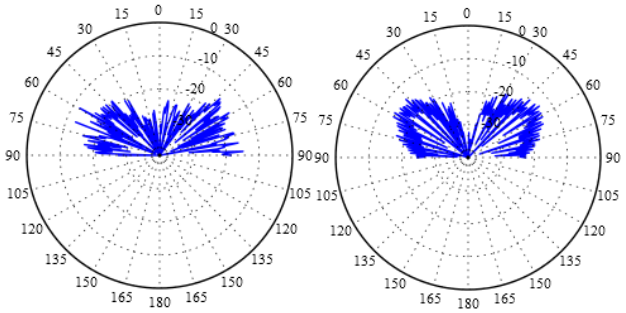

(a) 18 GHz (b) 27 GHz

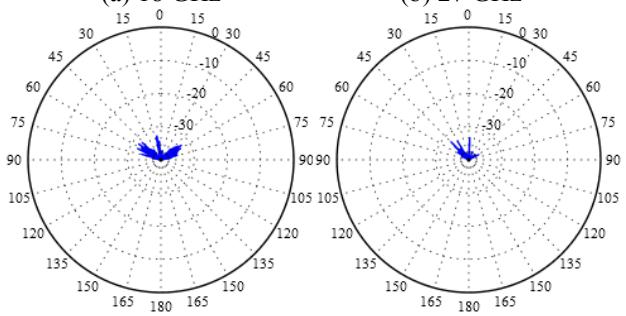

(a) 36 GHz (b) 45 GHz

Figure 14 – Amplitude error (in dB) between measurements with OEWG probes and the QRH.

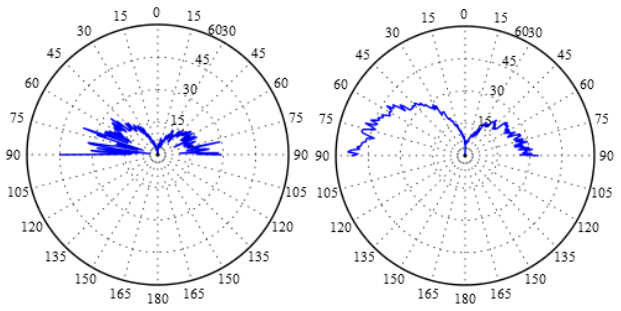

(a) 18 GHz (b) 27 GHz

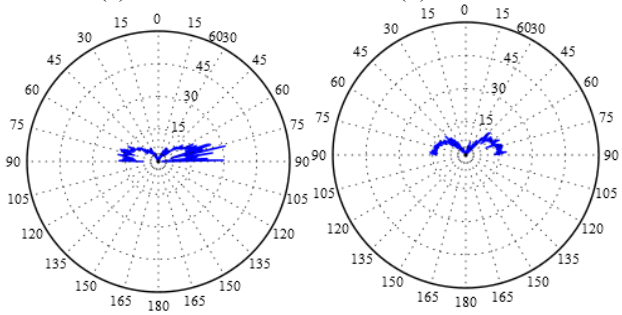

(a) 36 GHz (b) 45 GHz

Figure 15 – H-plane phase error (in degrees) between measurements with OEWG probes and the QRH.

5. Conclusions

This paper compared broadband unprocessed spherical near-field measurements conducted with three standard open-ended waveguide (OEWG) probes and a broad-band, broad-beam quad-ridged horn (QRH) antenna originally developed for towed decoy application. It was found that while the three OEWGs generally out perform the QRH in simulated pattern performance measures, measurements of a typical broad-beam AUT show only slight differences in the spherical near-field data. Therefore, for AUTs subtending an appropriately small solid angle of the probe, the QRH represents an alternative to typical OEWG probes for 18-45 GHz measurements.

9. Acknowledgements

This work was supported by the Office of Naval Research under grant #N00014-11-1-0818.

Table I – Summary of realized time savings using the University of Colorado antenna testing facility. The time for complete scan ranges from several minutes to several hours, depending on AUT.

OEWG	QRH
Mount WR-42 Probe (5 min)	Mount QRH Probe (5 min)
Scan (varies)	Scan (varies)
WR-42 to WR-28 Probe Change (5 min)	
Scan (varies)	
WR-28 to WR-22 Probe Change (5 min)	
Reconfigure Range Electronics (5 min)	Reconfigure Range Electronics (5 min)
Scan (varies)	Scan (varies)
Dismount Probe (5 min)	Dismount Probe (5 min)
Difference: (time for complete scan) + 10 min	
Scan time reduction: 33%	
Labor reduction: 40%	

8. References

[1] "NSI-700S-30 Spherical Near-field Measurement System Data Sheet." Nearfield Systems, Inc. available: http://ww2.nearfield.com/Sales/datasheets/pdfs/NSI-700S-30.pdf

[2] M. J. Radway and D. S. Filipovic, "Low-Cost Wideband 18-40 GHz Antenna with Consistent and Wide Radiation Patterns," *Proc. 2011 Antenna Applications Symp*., Monticello, IL, September 2011.

[3] J. E. Hansen, *Spherical Near-Field Antenna Measurements*, London: Peter Peregrinus Ltd., 1988.

[4] *High Frequency Structure Simulator (HFSS)*. ANSYS, Inc. available: http://www.ansys.com/Products/Simulation+Technology/Electromagnetics/High-Performance+Electronic+Design/ANSYS+HFSS

[5] M. J. Radway T. P. Cencich, and D. S. Filipovic, "Phase Center Stability of Planar Spiral Antennas," *Proc. 2009 Antenna Applications Symp*., Monticello IL, pp. 178-189, September 2009.